bioRxiv preprint doi: https://doi.org/10.1101/2021.02.01.429127; this version posted February 1, 2021. The copyright holder for this preprint (which was not certified by peer review) is the author/funder, who has granted bioRxiv a license to display the preprint in perpetuity. It is made available under a CC-BY 4.0 International license.

Identification of *Pectobacterium* species isolated from the soft rot of tetecho (*Neobuxbaumia tetetzo*), a columnar cactus, and associated metagenomics

David Vargas-Peralta[1¶], Delia A. Narváez-Barragán[2], Andrés de Sandozequi[2], Miguel F. Romero-Gutiérrez[3], Lorenzo Segovia[2], Claudia Martínez-Anaya[2*], Luis David Alcaraz[3] and Rodolfo de la Torre Almaraz[1¶]

[1]Unidad de Biotecnología y Prototipos, Facultad de Estudios Superiores Iztacala, Universidad Nacional Autónoma de México, Tlalnepantla, Estado de México, México.

[2]Departamento de Ingeniería Celular y Biocatálisis, Instituto de Biotecnología. Universidad Nacional Autónoma de México, Cuernavaca, Morelos, México.

[3]Departamento de Biología Celular, Facultad de Ciencias, Universidad Nacional Autónoma de México,Ciudad de México, México.

*Corresponding author

E-mail: claudia.martinez@mail.ibt.unam.mx (C. M.-A)

[¶]These authors contributed equally to this work.

bioRxiv preprint doi: https://doi.org/10.1101/2021.02.01.429127; this version posted February 1, 2021. The copyright holder for this preprint (which was not certified by peer review) is the author/funder, who has granted bioRxiv a license to display the preprint in perpetuity. It is made available under a CC-BY 4.0 International license.

Abstract

Neobuxbaumia tetetzo, commonly known as tetecho, is a columnar cactus endemic to Mexico. In the last 15 years, damage has been observed in young and adult plants of *N. tetetzo*, ranging from chlorotic spots with a wet appearance in early stages to tissue necrosis in advanced stages and finally the death of the plant; *Pectobacterium brasiliense* is the causal agent of the damages. Disease progression may be delayed or accelerated by the involvement of other bacteria, either pathogenic or endophytic, at the site of infection. Our goal was to confirm the presence of *Pectobacterium brasiliense*, in the soft rot of *N. tetetzo* and to determine the presence of other bacteria associated with the rot. We isolated three bacterial strains (A1, A3 and A8) from diseased tissue from three separate *N. tetetzo* plants, and compare them using biochemical and molecular techniques, such as whole-genome sequencing of strains A1 and A3. Phylogenetic analyzes confirmed that A1 corresponded to *P. brasiliense*, whereas A3 was more misimlar to *P. polaris*. Additionally, sequencing of 16S rRNA gene from metagenomic DNA isolated from healthy and diseased tissue of *N. tetetzo* indicated the presence of four operational taxonomic units (OTUs) at the order level, unique to the diseased tissue: Actinomycetales, Burkholderiales, Caulobacterales, and Sphingomonadales, with probable participation in the soft rot process.

bioRxiv preprint doi: https://doi.org/10.1101/2021.02.01.429127; this version posted February 1, 2021. The copyright holder for this preprint (which was not certified by peer review) is the author/funder, who has granted bioRxiv a license to display the preprint in perpetuity. It is made available under a CC-BY 4.0 International license.

Introduction

The Tehuacán-Cuicatlán Valley, Mexico, is a semi-arid zone covering an area of almost 10,000 km^2, it is considered one of the dry areas with the greatest diversity of flora and fauna, in addition to hosting a large number of endemic species. One endemic group of plants that stand out are the columnar cacti (Pachycereeae tribe) [1,2]. Zapotitlán de las Salinas is a community within the valley (18º20´N, 97º28´W), which houses the endemic columnar cactus *Neobuxbaumia tetetzo*, commonly called tetecho or teteche, forming dense forests of up to 1,200 individuals per hectare known as tetecheras. These tetecheras are of outmost importance for local inhabitants, since they are used as living fences, construction materials, firewood, food and ornamental plants, and are also of ecological relevance since they interact with different types of pollinators [3-5]. Observations of the last 15 years document plant damage and disease as follows: a) development of wet-looking chlorotic spots that may appear at the base, in the middle or in the upper part of the plant; b) spots turn gray; c) in advanced stages of the disease the tissue cracks and exudes a brown fluid; d) flesh detachment occurs exposing the woody tissue, and what is left dries out acquiring a dark gray aspect; eventually the plant may collapse (Fig 1).

Fig 1. Progression of soft rot in *N. tetetzo*. The onset of rot begins with wet-looking chlorotic spots (A); these spots turn gray (B and B¹); in advanced stages tissue loss and brown exudates occur (C); finally, the plant dries out and dies (D).

Damage is mainly attributed to the phytopathogenic bacteria *Pectobacterium carotovorum* subsp. *brasiliense* (now to elevated to the species *P. brasiliense*), identified by Mejía-Sánchez and collaborators (2019). The authors characterised 10 out of 80 isolates using pathogenicity and biochemical tests, comparison of the partial sequence of the 16S rRNA gene against the nt database of GenBank, amplifing the intergenic spacer region (ISR) 16S-23S rRNA with the BR1f / L1r oligonucleotides [7], and phylogenetic reconstruction using multiple alignments of the sigma factor 38 of the RNA polymerase subunit (*rpoS*). Although analysis of the 16S rRNA gene and the *rpoS* gene are a first aproach for species identification [8], more information can be used for better taxonomic resolution either at the species or subspecies level. Although the region amplified by the BR1f / L1r oligonucleotides is

bioRxiv preprint doi: https://doi.org/10.1101/2021.02.01.429127; this version posted February 1, 2021. The copyright holder for this preprint (which was not certified by peer review) is the author/funder, who has granted bioRxiv a license to display the preprint in perpetuity. It is made available under a CC-BY 4.0 International license.

specific for *P. brasiliense*, it lacks evidence to confirm the presence of the *P. brasiliense* in *N. tetetzo*, but provides a first approximation.

Disease progression may be delayed or accelerated by the involvement of other bacteria, either pathogens, or endophytes that under certain conditions are able to participate in the development of symptoms [9][10]. The use of classical microbiology techniques coupled with Next Generation Sequencing (NGS) technologies to obtain partial or complete sequences of bacterial genomes, allows better characterization of new bacterial isolates from *N. tetezo* providing better support and resolution for bacterial taxonomy [8]. NGS technologies also aid in the analysis of microbial populations and communities [11], to understand the participation of two or more bacteria and their contribution to the occurrence of plant diseases. We aimed to confirm the presencie of *Pectobacterium brasiliense* during *N. tetetzo* soft rot and to explore the bacterial diversity associated with the pathology of this impostant cactus.

Materials and methods

Tissue collection and isolation of *Pectobacterium* sp.

Two samples of healthy and diseased tissue from *N. tetetzo* from the Zapotitlán de las Salinas region were collected. Potatoes were used as bait in the first sampling to isolate the primary causative agent, *Pectobacterium* sp. A total of four potatoes were inoculated, three with diseased tissue and one with healthy tissue (control). Rotten potato tissue was scraped and streaked in Petri dishes with nutrient agar medium (Merk), incubated at 37 ° C for 48 h, several passes were performed under the same conditions until isolated colonies were obtained. Three *Pectobacterium* sp isolates were obtained, and assigned the names A1, A3 and A8. In the second sampling, healthy and diseased tissue from *N. tetetzo* was taken with a perforation tool and placed in sterile centrifuge tubes and transported to the laboratory.

Phenotypic characterization

Biochemical tests were performed according to Schaad et al. (2001) for the identification of phytopathogenic bacteria, including: Gram stain, KOH test, anaerobic growth in Hugh and Leifson medium, mucoid colonies in

bioRxiv preprint doi: https://doi.org/10.1101/2021.02.01.429127; this version posted February 1, 2021. The copyright holder for this preprint (which was not certified by peer review) is the author/funder, who has granted bioRxiv a license to display the preprint in perpetuity. It is made available under a CC-BY 4.0 International license.

yeast extract-dextrose-CaCO3 (YDC) medium, yellow or orange colonies in YDC and Nutrient-broth yeast extract agar (NBY) and fluorescence in King B medium (KB). Three repetitions per isolate (A1, A3 and A8) were performed for each test.

Pathogenicity tests and host range

Plant material was previously disinfected with 5% sodium hypochlorite and rinsed with distilled water. From fresh Petri dish cultures of the three isolates, colonies were taken and diluted in phosphate buffer pH 7.4 at OD_{600}=0.4 ($1x10^{32}$ cells), each *N. tetetzo* plant of approximately four years old was inoculated with 3-ml syringes. Host range was tested in other Cactaceae species: *Opuntia ficus-indica* cladodes (prickly pear) and *Pachycereus pringlei* (elephant cactus). Six squares (2 cm each side) were traced on cladodes of *Opuntia ficus-indica*, four of them were inoculated with 500 µL of the bacterial suspension and the remaining two were inoculated with 500 µL phosphate buffer and sterile H_2O as controls. Cladodes were incubated under greenhouse conditions for 17 days. *P. pringlei* were inoculated by duplicate, in a small cut with 10 µl bacterial suspension ($1x10^8$ cells) per isolate from overnight cultures in LB medium and incubated in a humid chamber at 30°C for 24 h.

Determination of virulence

Virulence was determined as the extent of plant tissue degradation and quantified by tissue loss on celery stalks. Five-mm cuts on disinfected (with 5% sodium hypochlorite for 15 min) celery stalks pieces of approximately 15 cm, were inoculated with 10 µl of diluted to OD_{600}=0.1 the different isolates overnight cultures in LB medium (n=33 per strain). These were incubated in a humid chamber at 30ºC for 24 h. Tissue loss was determined by the difference of weight before and after removing the macerated tissue.

Detection of plant cell wall degrading enzymes (PCWDE's)

Enzymatic activity was detected in plate assays. LB agar medium (Bacto) was prepared with 2% sodium carboxymethyl cellulose (CMC) (Merck) or 2% pectin (Agdia AG366) prepared according to the provider instructions; bacteria were plated 30 min after pouring the media. A drop of 3 µL of each strain diluted to OD_{600} = 0.1 was placed in the center the Petri dish on both substrates (by triplicate), allowed to dry for 20 min and incubated in a humid chamber at 30ºC for 48 h. Enzymatic activity towards CMC was revealed with Congo red

bioRxiv preprint doi: https://doi.org/10.1101/2021.02.01.429127; this version posted February 1, 2021. The copyright holder for this preprint (which was not certified by peer review) is the author/funder, who has granted bioRxiv a license to display the preprint in perpetuity. It is made available under a CC-BY 4.0 International license.

1% for 15 min, then rinsed with 1 M sodium chloride. Pectinolytic activity was detected with 0.1% toluidine blue for 10 min and washed with 20 mM HEPES pH 7.5. Enzymatic index (EI) was calculated by dividing the hydrolysis halo by the colony halo [13].

Identification of strains A1, A3 and A8

End-point PCR targeting of the 16S rRNA gene.

Genomic DNA was extracted using the modified method of Dellaporta et al. (1983), for PCR (Taq DNA polimerase recombinant, Invitrogen) reactions with oligonucleotides FD1 (5' AGAGTTTGATCCTGGCTCAG 3') and RD1 (5' AAGGAGGTGATCCAGCC 3') for a 1,600 bp amplicon [15]. PCR set up was: 94ºC / 3 min, 30x (94 ° C / 1 min, 55ºC / 30 s, 72ºC / 2 min) and 72ºC / 7 min. PCR products were purified (Wizar SV kit, Promega), and sequenced (at the FESI-UNAM Molecular Biochemistry Laboratory), for comparison against the non-redundant nucleotide database (Nucleotide collection, nr/nt) of the GenBank (NCBI), using BLASTn [16,17], with Megablast program, with a cut-off value of E from 1 to 6, a word size of 28 and a mismatch score of -2.

Genome sequencing, annotation and comparative genomics

Strains A1 and A3 obtained from the first field sampling were selected for genome sequencing at the UUSMD, Instituto de Biotecnología-UNAM. Sequencing quality was analyzed with the free software FastQC High Throughput Sequence QC Report, version 0.11.7 https://www.bioinformatics.babraham.ac.uk/projects/download.html. Genome were assembled with Velvet version 1.2.10 [18], using a sweep (33 > K < 53) to select the best K value for each draft genome. K-value was selected with QUAST program [19]. Draft genomes were annotated with Prokka v1.11 program [20]. Venn diagram was constructed as previously described in [21]. Predicted proteins of strains A1 and A3 were compared to reference genomes of *P. brasiliense* BC1 (NZ_CP009769.1) and *P. polaris* NIBIO1392 (NZ_CP017482.1), and against each other (all-vs-all BLAST) with Proteinortho v5.16 using reported parameters (p-value $<10^{-5}$, identity >35%, and match lengths >75%) [22]. Subsystem assignment, circular genome construction, and virulence, transport and antibiotic resistance genes were predicted with PATRIC suit [23].

bioRxiv preprint doi: https://doi.org/10.1101/2021.02.01.429127; this version posted February 1, 2021. The copyright holder for this preprint (which was not certified by peer review) is the author/funder, who has granted bioRxiv a license to display the preprint in perpetuity. It is made available under a CC-BY 4.0 International license.

Phylogenetic analysis

For comparison genomics two analyzes were used: Pyani python average nucleotide identity (ANI) module using the BLAST algorithm (ANIb) [24], with 100 *Pectobacterium* genomes (available until march of 2018, S1 Table), with a suggested cut-off value of 95-96% to delimit bacterial species; the second analysis was based on coding sequences (CDS) of 120 genomes (113 genomes of *Pectobacterium* sp and 5 genomes of the genus *Yersinia* (available until october of 2018; S1 Table) for the construction of a phylogenetic tree, for this the distance measurement between species was established with a Genomic Similarity Score (GSS) based on the sum of the bit scores of shared orthologs, detected as Reciprocal Best Hits (RBH), normalized against the sum of the bit scores of the genes compared against themselves (scores of own bits). The GSS varies in values from 0 to 1, where all the orthologous proteins between two proteomes that are identical has a maximum value of 1, on the contrary, when two proteomes do not show similarity in orthologous proteins, it has a value of 0 [25], the GSS matrix was converter using the expresing 1-GSS, from this, a distance matrix of the GSS scores of the shared orthologs for the proteomes used in a Neighbor-Joining tree is drawn to visualize the genomic distance between the isolates; the tree was built from 1,000 replicas [26].

Massive sequencing of amplicons of the 16S rRNA gene from samples of *N. tetezo*

For a second sample collected, metagenomic DNA was extracted using the DNAzol® Reagent kit (Invitrogen) from healthy and diseased tissue from *N. tetetzo*, and massive sequencing of the 16S rRNA gene of the V3 and V4 hypervariable regions was performed at the UUSMD Unit-IBT, UNAM, by pair-end sequencing in an Illumina NextSeq® 500 sequencer. For the processing of the sequences, the pipeline was followed according to the Standardized Operating Protocols (SOP) Environmental Genomics FC-UNAM (http://genomica.fciencias.unam.mx/github/). Briefly, the quality of the sequences was visualized with the FastQC High Throughput Sequence QC Report software, version 0.11.7. [27]; quality control and alignment of the readings were performed using the CASPER software [28]. With QIIME program, *subsample_fasta.py* random sequences were taken from the files to be analyzed. Grouping and selection of Operational Taxonomic Units (OTUs) were

bioRxiv preprint doi: https://doi.org/10.1101/2021.02.01.429127; this version posted February 1, 2021. The copyright holder for this preprint (which was not certified by peer review) is the author/funder, who has granted bioRxiv a license to display the preprint in perpetuity. It is made available under a CC-BY 4.0 International license.

performed using the CD-HIT-EST [29] program with an identity cut-off 97%, and representative sequences were selected with the option *pick_rep_set.py* from QIIME. Sequence filters used a first matching against the Greengenes database (gg_13_8_otus; 70% OTUs) eliminating sequences without 16S matches. Matched sequences (70% OTUs) were the input of taxa annotation (97% OTUs Greengenes). The OTUs table was constructed using the QIIME *make_otu_table.py* option, chimeras were identified and eliminated with ChimeraSlayer [30-32] mitochondrial, and chloroplast sequences were also identified and removed. Finally, graphs were constructed using R version 3.5.3 sofware with the help of the Phyloseq data package [33].

Results

Isolation and Phenotypic characterization of *Pectobacterium sp.* from *N. tetezo*

We have preoviusly reported that *P. brasiliense* causes soft rot in *N. tetetzo* [6], but here we aimed to analyse new isolates in more detail. Using potatoes as baits to collect samples of three diseased and healty individuals we confirmed rot of potatos inoculated with infected cactus tissue while potatoes inoculated with healthy tissue did no rot. Three strains were isolated and designated as A1, A3 and A8 presented the following phenotype: they were negative for Gram staining and positive for the KOH test, thus they are Gram-negative bacteria. All are facultative anaerobic bacteria due to turning Hugh and Leifson medium from blue to yellow. None formed mucoid colonies at 30°C in YDC medium, nor formed yellow or orange colonies in YDC and NBY, respectively, and did not fluoresce in KB medium. Contrarily, all isolates grew well in pectin-containing medium.

Pathogenicity tests and host range

To determine if the isolates caused sooft rot, young *N. tetetzo* plants were inoculated with each strain. Indeed, all the strains reproduced the symptoms observed in wild cacti: on day one, infected plants presented a slight loss of turgidity, the tissue cracked and exuded a brown fluid. On day two, loss of turgor was more noticeable, the tissue began to darken and the brown liquid continued to emerge, these symptoms worsened as time went on. On day

bioRxiv preprint doi: https://doi.org/10.1101/2021.02.01.429127; this version posted February 1, 2021. The copyright holder for this preprint (which was not certified by peer review) is the author/funder, who has granted bioRxiv a license to display the preprint in perpetuity. It is made available under a CC-BY 4.0 International license.

183 fifteen, inoculated plants lost turgidity, developed a gray-green color and desiccated, indicating their death (Fig
184 2). These results confirmed that our strains do correspond to the etiological agent of sooft rot.
185
186 **Fig 2. Progressive damage of *N. tetetzo* inoculated with strains A1, A3 and A8.** The time from inoculation to
187 plant death is indicated at the top. On the left side the name of the isolates and the control. Only strains A1 and A3
188 are presented. Top row shows cactus inoculated with strain A1. The second row corresponds to cactus inoculated
189 with strain A3; both isolates caused loss of turgidity, liquid runoff, tissue darkening, desiccation and plant death
190 in a similar period. Third row is a control cactus inoculated with sterile H_2O that did not show damage during the
191 experiment duration.
192
193 We then analyzed whether our strains provocked disease only in *N. tetezo* or whether they are virulent in other
194 cactaceous species: *Opuntia ficus-indica* and *Pachycereus pringlei.* Inoculation of strains in *O. ficus-indica*
195 cladodes developed a wet-looking chlorotic spot at 6 days post-inoculation (dpi); at nine dpi chlorotic spots turned
196 brownish-green, with a brwon necrotic margin; by 12 dpi the spots turned brown, and finally at 17 dpi they
197 darkened, some of spots cracked and exuded a dark fluid. The section inoculated with sterile H_2O was intact for
198 the duration of the expetiment. Again, the symptoms provoked in *O. ficus-indica* were similar to those observed
199 in the field in *N. tetetzo* (Fig. 3). Finally we analyzed infection of *P. pringlei*. Because individuals of this species
200 were quite small, the bacteria inoculum size was smaller than that used in the previous experiments; this allowed
201 observing differences of virulence between isolates: A1 and A8 showed tissue maceration at one dpi, and at 2 dpi
202 infected plants already showed signs of severe rot and total loss of turgor; meanwhile plants inoculaed with isolate
203 A3 showed a delay of tissue maceration in comparison to A1 and A8, as rot was detected only at 2 dpi. Control
204 plants inoculated with LB medium remained healthy during the time of the experiment (Fig 4). Taken together,
205 these results confirm that strains A1, A3 and A8 recapitulate *in vitro* the disease symptoms observed in wild tetecho
206 cacti, and they point to *Pectobacterium* as the ethiological agent, in agreement to previous observations [6].
207
208 **Fig. 3. Progressive damage to *Opuntia ficus-indica*.** Only isolate A1 is presented. In panel (**A**), prickly pear
209 cactus cladode shows all 6 (2x2 cm) squares, four of which were inoculated with strain A1 and the two remaining

bioRxiv preprint doi: https://doi.org/10.1101/2021.02.01.429127; this version posted February 1, 2021. The copyright holder for this preprint (which was not certified by peer review) is the author/funder, who has granted bioRxiv a license to display the preprint in perpetuity. It is made available under a CC-BY 4.0 International license.

squares were inoculated with phosphate buffer pH 7.4 and sterile H_2O, respectively. In panel (**B**), the top row shows the appearance of symptoms of one infected area through the time, in comparison to the bottom control treatment (with H_2O) indicated on the right.

Fig 4. Progressive infection symptoms in *P. pringlei*. Control treatment left is compared with strains A1, A3 and A8 inoculation, through the time (top to bottom).

Virulence determination and PCWDEs

Given the previous result showing differences between strains, we aimed to compare their virulence in more detail. We used celery stalks as a laboratory model, given its availability and fast symptoms development after inoculation with *P. brasiliense* in comparsion to cacti [34]. We quantified virulence as the amount of tissue loss due to degradation. We found that, similarly to the observed phenotype in *P. pringlei*, isolates A1 and A8 produced more extensive rot in celery (20%) with respect to the isolate A3 (5%) under the same experimental conditions (Fig 5), confirming a different capacity to degrade the plant material between strains. Plant degradation by *Pectobacterium* is due to different plant cell wall degrading enzymes (PCWDEs), thus we asked whether the enzynatic activities between strains also differ. Using a plate assay, we found that the three strains produced halos of comparable size in CMC- and pectin-containing media (Table 1) suggesting that the difference in virulence between strais is independent of their degrading capacity, although it is necessary to analyse individual enzymes produced during infection and other virulence factors.

Fig 5. Infection phenotypes in celery. Panel (**A**), phenotypes of infection by strains A1, A3 and A8 compared to inoculation with LB medium control "C". Panel (**B**), quantification of tissue loss in celery caused by each strain. *$p \leq 0.005$.

bioRxiv preprint doi: https://doi.org/10.1101/2021.02.01.429127; this version posted February 1, 2021. The copyright holder for this preprint (which was not certified by peer review) is the author/funder, who has granted bioRxiv a license to display the preprint in perpetuity. It is made available under a CC-BY 4.0 International license.

Table 1. Plaque enzyme activity

Substrate	Strain	Enzyme index (EI) in cm
Carboxymethyl cellulose (CMC)	A1	2.67
	A3	2.5
	A8	2.67
Pectin	A1	2.47
	A3	2.33
	A8	2.47

Molecular characterization of strains A1, A3 and A8, phylogenetic analysis and comparative genomics

Molecular identification.

To confirm the identity of strains A1, A3 and A8 we first analysed the 16S rRNA gene sequence, indicating the following identities: A1 (MG008909.1) and A8 (MG008910.1) were 97% identical to *P. brasiliense* and 100% *P. carotovorum*, respectively. While A3 (MN216189.1) was 98% identical to *P. polaris* and 100% identical to *P. brasiliense*. For a more precise identification we obtained the draft genome of strains A1 and A3 (S1 Figure) (data avaliable in the bioproject PRJNA669375). The two genomes were assembled and annotated (Table 2).

Table 2. Data generated from the assembly and annotation of the isolates

Feature	Isolates	
	A1	A3
Total number of contings	381	326
Largest contig	124 352	263 985
N50	46 958	59 089
L50	32	26
% GC	52.31	51.96
Genome size in bp	4 500 321	4 873 548
Coding sequences (CDS)	4 013	4 334
tRNA	32	36
rRNA	3	3
Transfer-messenger RNA (tmRNA)	1	1
Hypothetical proteins[P]	736	859
Proteins with functional assignments[P]	3715	3922

bioRxiv preprint doi: https://doi.org/10.1101/2021.02.01.429127; this version posted February 1, 2021. The copyright holder for this preprint (which was not certified by peer review) is the author/funder, who has granted bioRxiv a license to display the preprint in perpetuity. It is made available under a CC-BY 4.0 International license.

Proteins with EC number assignments[P]	1107	1123
Proteins with GO assignments[P]	918	932
Proteins with Pathway assignments[P]	812	815
Antibiotic Resistance[P]	44	42
Virulence Factor[P]	46	59

[P]Predicted with PATRIC suite

Phylogenetic analysis

According to the ANI analysis, the similarity value between the isolates obtained from *N. tetetzo*, A1 vs A3 was 93.9% below the cut-off value 95-96%, so they are different species (S2 Table). Isolate A1 had an average of 97.1% similarity when compared against 29 *P. brasiliense* genomes, above the cut-off value. When compared to 5 *P. polaris* genomes and 9 *P. carotovorum* genomes, A1 had an average similarity value of 93.9% and 93.3% respectively (S2 Table). Isolate A3 had an average of 96.7% similarity when compared against 5 *P. polaris* genomes, above the cut-off value. When compared against 29 genomes of *P. brasiliense* and 9 genomes of *P. carotovorum*, it had an average similarity value of 94% and 93.3% (S2 Table), respectively (Fig 6). By using another metric such as the genomic similarity score tree (GSS), the tree in this analysis showed three well-defined groups (Fig 7). Group 1 is formed by *Pectobacterium fontis*, a distant species from other *Pectobacterium* because it is shared as a sister clade of groups 2 and 3. Group 2, including *P. betavasculorum*, *P. wasabiae, P. parmentieri*, *P. peruviense*, *P. atrosepticum,* and *P. punjabense*, formed supported and unique subgroups. Finally, Group 3 formed a supported group, with a subgroup including *P. versatil* sp. nov., and *P. odoriferum* sp. nov.; *P. polaris* and *P. brasiliense* are sister groups. To our surprised strain A1 grouped with *P. brasiliense* while strain A3 clustered with *P. polaris*. These results (ANI and GSS) confirmed the identity of *P. brasiliense* for strain A1, and revealed the identity of strain A3 as *P. polaris*, possibly explaining the differences observed by biochemical and pathogenicity tests of each strain.

Comparative genomics

We then compared A1 and A3 with the reference strains *P. brasiliense* BC1 and *P. polaris* NIBIO1392, with which they are grouped. We found that the four strains share a nucleus of 3,724 coding sequences (CDS). Strains A1 and

bioRxiv preprint doi: https://doi.org/10.1101/2021.02.01.429127; this version posted February 1, 2021. The copyright holder for this preprint (which was not certified by peer review) is the author/funder, who has granted bioRxiv a license to display the preprint in perpetuity. It is made available under a CC-BY 4.0 International license.

A3 shared 108 CDSs, most of which are associated with membrane transport. Strain A1 contains 343 unique CDS that participate in membrane transport, energy and generation of metabiolite precursors. Compared with the reference strains, A1 shared 192 CDS with *P. brasiliense* BC1, and 14 CDS with *P. polaris* NIBIO1392. Strain A3 contains 288 unique CDS, mostly associated with membrane transport. And the comparison to the reference strains showed that A3 shares 55 CDS with *P. brasiliense* and 360 CDS with *P. polaris* (Figure 8). Again, this results indicate that A1 and A3 are different species.

Fig 6. Heatmap of ANI percentage identity for isolates of *Pectobacterium* strains.

Heatmap corresponding to 95% ANIb sequence identity are colored red. Blue cells correspond to ANIb comparisons of organisms that do not belong to the same species. Species in the groups formed is indicated on the right side. One asterisk indicates the position of strain A1, and the double asterisk shows the position of strain A3.

Fig 7. Genomic Similarity Score (GSS) matrix plotted as Neighbor-Joining tree. This tree shows the relationship between isolates A1 and A3 and other *Pectobacterium* species from the comparison of the entire proteome. *Yersinia sp*. Was included as an external group. The consensus tree was inferred from 1,000 replicates. The asterisk (*) indicates the position of strains A1 and A3.

Fig 8. Comparison strains A1 and A3 with two *Pectobacterium* reference genomes. Venn diagram representing the whole genome comparison of sequenced *Pectobacterium* strains A1 and A3, and two complete reference genomes (*P. brasiliense* BC1 and *P. polaris* NIBIO1392). Numbers indicate shared coding sequences (CDS) between strains. Pie charts plot the number of CDS assigned to a main functional role category (subsystem), hypothetical proteins and unknown or unassigned sequences.

N. tetetzo microbiome in health and disease

Finally, we investigated other bacteria that could be participating in the disease course of *N. tetetzo* besides *Pectobacterium*, as it is known for other hosts that as the infection progresses, the microbial community changes. Thus, we analyzed the bacterial community found in an diseased individual and compare it with a healthy cactus. We used metagenomic DNA to describe the microbiome by means of the variable region of the 16S rRNA sequencing. Healthy tissue of *N. tetetzo* contained only three OTUs, assigned at the order level to: Lactobacillales,

bioRxiv preprint doi: https://doi.org/10.1101/2021.02.01.429127; this version posted February 1, 2021. The copyright holder for this preprint (which was not certified by peer review) is the author/funder, who has granted bioRxiv a license to display the preprint in perpetuity. It is made available under a CC-BY 4.0 International license.

Oceanospirillales (being the predominant) and Rhizobiales. In comparison, diseased tissue showed greater abundance of OTUs, including: Actinomycetales, Burkholderiales, Caulobacterales, Lactobacillales, Oceanospirillales, Rhizobiales and Sphingomonadales; here, similarly to the healthy sample, the orders Lactobacillales and Oceanospirillales were predominant (Figure 9).

Figuere 9. Orders detected in *N. tetetzo* tissue. Three bacterial orders were detected in healthy tissue of *N. tetetzo*: Lactobacillales, Oceanospirillales and Rhizobiales. The orders detected in diseased tissue were: Actinomycetales, Burkholderiales, Caulobacterales, Lactobacillales, Oceanospirillales, Rhizobiales and Sphingomonadales. Healthy tissue is less diverse than diseased tissue.

Discussion

Characterization of *Pectobacterium* sp.

Here, we give evidence of *Pectobacterium* as the etiological agent of the soft rot of *N. tetetzo*, in agreement with the report of Mejía-Sánchez and collaborators (2019). Biochemical testing indicated identical profiles for three strains isolated from rotten cacti, and the 16S-rRNA gene established that all three belong to the *Pectobacterium* genus. However, further whole genome analyses of A1 and A3, indicated that they are different species: A1 groups with *P. brasiliense* whereas A3 seems to be *P. polaris*, which represents a surprising result. *P. brasiliense* was first reported in Brazil in 2004 by Duarte and collaborators and since then it has reached all continents; meanwhile *P. polaris* was reported in Norway and Poland only recenlty (in 2017). The presence of *Pectobacterium* in different parts of the world, including an isolated area such as Zapotitlán de las Salinas, Puebla is proof that it is a highly mobile ubiquitous pathogen probably present due to globalization. That A1 (and possibly also A8) and A3 are different species could explain the difference on symptom onset that we oberved for each of them. Despite the maceration delay by A3 in comparison to A1 and A8, all isolates caused infection in the hosts analysed: celery and three types of cacti, *O. ficus-indica, N. tetetzo* and *P. pringlei*, adding these to the list of plants susceptible to *Pectobacterium* infection. To our best knowledge, this would represent the first report of *P. polaris* capability for

bioRxiv preprint doi: https://doi.org/10.1101/2021.02.01.429127; this version posted February 1, 2021. The copyright holder for this preprint (which was not certified by peer review) is the author/funder, who has granted bioRxiv a license to display the preprint in perpetuity. It is made available under a CC-BY 4.0 International license.

313 infecting cacti, besides potato [35]. These differences found in maceration capacity are mainly due to the fact that
314 they are two different species according to our phylogenetic analyzes, ANI and GSS, where isolate A1 is grouped
315 with *P. brasiliense* and isolate A3 with *P. polaris*; the ANI pattern agrees with the data presented by Narváez-
316 Barragán and collaborators 2020, while our GSS tree presents a topology similar to that presented by Portier and
317 collaborators (2019). The main advantage of GSS is that it uses both core and pan-genomic information to estimate
318 relatedness between strains. Proteins are the preferred choice to find homologs with large evolutionary distances
319 [37], allowing a better resolution when working with genres.
320 *Pectobacterium* sp. has also been reported as the main etiological agent of rot in commercial crops in Baja
321 California of prickly pear cactus, *O. ficus-indica* [38]. This is important because Mexico is the main producer and
322 consumer of *O. ficus-indica*, since around 72,000 ha of the country are cultivated to produce fruit and
323 approximately 10,500 ha are cultivated for vegetable production purposes, which is carried out in most of the
324 country's states [39,40], knowing the identity of the pathogen in these crops is essential for establishing adequate
325 sanitary measures to minimize crop losses.
326 Few articles have reported the presence of *Pectobacterium* in wild plants, in this case *N. tetetzo*, *P. pringlei*
327 (although no symptoms have been observed in the field) and in *Carnegiea gigantea* [41], which indicates that we
328 know very little of the ecological function of this pathogen in arid areas where these columnar cacti are found.

329 *N. tetetzo* microbiome in health and disease

330 Finally, our analysis of the bacterial community composition during infection of *N. tetetzo* allowed the
331 identification of different OTUs, however *Pectobacterium* was absent at this disease stage. This was surprising
332 but not unexpected, as infections are dynamic processes in which drastic changes of the bacterial community can
333 occur, specially in long-term infection such that observed in *N. tetetzo*. In support to our observations, Kõiv and
334 collaborators (2015) examined the changes of the endophytic bacterial community in potato tuber (*Solanum*
335 *tuberosum*) in response to infection by *P. atrosepticum* finding that eight days after inoculation, the
336 Enterobacterales order either decreases or disappears, and others with cellulolytic/pectinolytic capacity such as the
337 Clostridiales appear. This report indicates that although *P. atrosepticum* initiates the infection, it provides a niche
338 for the potato endophytes that then contribute to the degradation of different components of the plant, many of

bioRxiv preprint doi: https://doi.org/10.1101/2021.02.01.429127; this version posted February 1, 2021. The copyright holder for this preprint (which was not certified by peer review) is the author/funder, who has granted bioRxiv a license to display the preprint in perpetuity. It is made available under a CC-BY 4.0 International license.

339 them being opportunists. This seems to be the case also for *N. tetetzo*, which in the absence of infection supports
340 a limited community including the orders Lactobacillales, Oceanospirillales and Rhizobiales. In agreement with
341 our observations, Lactobacillales have been reported in the stem endosphere of other cacti, such as
342 *Myrtillocactus geometrizans* and *Opuntia robusta* [43]. Oceanospirillales are generally halophilic marine bacteria,
343 but their presence could be the result of the complex history of the Tehuacán-Cuicatlán valley, which includes
344 deposition events of salt-rich marine sediments during the lower Cretaceous. However, at more advance disease
345 stages the community diversifies including OTUs from the orders: Actinomycetales, Burkholderiales,
346 Caulobacterales and Sphingomonadales, of which the Actinomycetales stand out as being decomposers of organic
347 matter, contributing to the rot of *N. tetetzo*. Another important order is Burkholderiales since some of these can be
348 pathogens in plants, including species such as *Burkholderia* and *Ralstonia*, in addition to being natural inhabitants
349 of the soil [44]. Caulobacterales have been reported in very diverse habitats, mainly aquatic, in the soil and on the
350 surfaces of eukaryotes, they even form biofilms that allow them to withstand adverse periods, it has also been
351 reported that these bacteria are the main degraders of macroscopic organic aggregates and the release of amino
352 acids to be consumed by other bacteria [45,46], thus probably participating in the rot.

353 # Conclusions

354 Isolates A1 and A8 were more virulent with respect to isolate A3, because they are different species. In the same
355 way, the presence of *Pectobacterium brasiliense* and another species of *Pectobacterium*, *Pectobacterium polaris*
356 in the soft rot of *N. tetetzo* was confirmed.
357 The genome of isolate A1 (*P. brasiliense*) presented a percentage of guanin-cytosine (%GC) of 52.31, 4,013
358 coding regions, N50 of 46,958 and an approximate genome size of 4,500,321 bp, while the genome of isolate A3
359 (*P. polaris*) presented a %GC of 51.96, 4,334 coding regions, N50 of 59,089 and an approximate genome size of
360 4,873,548 bp.
361 The microbiome analysis revealed three main OTUs in healthy tissue from *N. tetetzo*: Lactobacillales,
362 Oceanospirillales, and Rhizobiales. Also we detected four OTUs in diseased tissue other than healthy:
363 Actinomycetales, Burkholderiales, Caulobacterales, and Sphingomonadales.

bioRxiv preprint doi: https://doi.org/10.1101/2021.02.01.429127; this version posted February 1, 2021. The copyright holder for this preprint (which was not certified by peer review) is the author/funder, who has granted bioRxiv a license to display the preprint in perpetuity. It is made available under a CC-BY 4.0 International license.

Acknowledgements

The first author would like to thank Consejo Nacional de Ciencia y Tecnología for the Grant (number 816227) that supported his Master degree, and Posgrado de Ciencias Biológicas of Universidad Nacional Autónoma de México (UNAM).

Funding Information

This project was financed by grants from DGAPA-PAPIIT (IN216317) and CONACYT (A1-S-33379) to R .T.A. And DGAPA-PAPIIT (IN211019) and CONACYT Ciencia Básica (252551) to C. M.-A.

bioRxiv preprint doi: https://doi.org/10.1101/2021.02.01.429127; this version posted February 1, 2021. The copyright holder for this preprint (which was not certified by peer review) is the author/funder, who has granted bioRxiv a license to display the preprint in perpetuity. It is made available under a CC-BY 4.0 International license.

References

1. Dávila P, Arizmendi MDC, Valiente-Banuet A, Villaseñor JL, Casas A, & Lira R. Biological diversity in the Tehuacán-Cuicatlán Valley, Mexico. *Biodiversity and Conservation*.2002;11(3):421-442. doi: https://doi.org/10.1023/A:1014888822920

2. Valiente-Banuet A, Arizmendi MDC, Rojas-Martínez A, & Domínguez-Canseco L. Ecological relationships between columnar cacti and nectar-feeding bats in Mexico. J. Trop. Ecol. 1996;12(01):103-119. doi: https://doi.org/10.1017/S0266467400009330

3. Godínez-Álvarez HO. El tetecho: historia natural de una cactácea columnar del centro de México. Ciencia: Revista de la Academia Mexicana de Ciencias. 2001;52(1-2):52-57.

4. Valiente-Banuet A, Rojas-Martinez A, Arizmendi MDC, & Davila P. Pollination biology of two columnar cacti (Neobuxbaumia mezcalaensis and Neobuxbaumia macrocephala) in the Tehuacan Valley, central Mexico. Am. J. Bot. 1997;84(4):452-452. doi: https://www.jstor.org/stable/2446020

5. Valiente-Banuet A, Rojas-Martínez A, Casas A, del Coro Arizmendi M, & Dávila P. Pollination biology of two winter-blooming giant columnar cacti in the Tehuacan Valley, central Mexico. J. Arid Environ. 1997; 37(2): 331-341. doi: https://doi.org/10.1006/jare.1997.0267

6. Mejía-Sánchez D, Aranda-Ocampo S, Nava-Díaz C,Teliz-Ortiz D, Livera-Muñoz M, De La Torre-Almaráz R, et al. *Pectobacterium carotovorum subsp. brasiliense* Causes Soft Rot and Death of *Neobuxbaumia tetetzo* in Zapotitlan Salinas Valley, Puebla, Mexico. Plant Disease. 2019;103(3):398-403. doi: https://doi.org/10.1094/PDIS-02-18-0370-RE

7. Duarte V, De Boer S, Ward L. and Oliveira A. Characterization of atypical *Erwinia carotovora* strains causing blackleg of potato in Brazil. Journal of Applied Microbiology. 2004;96:535-545. doi:10.1111/j.1365-2672.2004.02173.x

8. Raina V, Nayak T, Ray L, Kumari K, Suar M. Chapter 9 - A Polyphasic Taxonomic Approach for Designation and Description of Novel Microbial Species. In: Das S, Dash HRBT-MD in the GE, editors. Academic Press; 2019. pp. 137–152. doi: https://doi.org/10.1016/B978-0-12-814849-5.00009-5

bioRxiv preprint doi: https://doi.org/10.1101/2021.02.01.429127; this version posted February 1, 2021. The copyright holder for this preprint (which was not certified by peer review) is the author/funder, who has granted bioRxiv a license to display the preprint in perpetuity. It is made available under a CC-BY 4.0 International license.

9. Suhaimi NSM, Goh S-Y, Ajam N, Othman RY, Chan K-G, Thong KL. Diversity of microbiota associated with symptomatic and non-symptomatic bacterial wilt-diseased banana plants determined using 16S rRNA metagenome sequencing. World J Microbiol Biotechnol. 2017; 33:168. doi: https://doi.org/10.1007/s11274-017-2336-0

10. Kõiv V, Roosaare M, Vedler E, Kivistik PA, Toppi K, Schryer DW., et al. Microbial population dynamics in response to *Pectobacterium atrosepticum* infection in potato tubers. Sci. Rep. 2015;5:11606. doi: https://doi.org/10.1038/srep11606

11. van Dijk EL, Auger H, Jaszczyszyn Y, and Thermes C. Ten years of next-generation sequencing technology. Trends Genet. 2014; 30: 418–426. doi: https://doi.org/10.1016/j.tig.2014.07.001

12. Schaad NW, Jones JB, Chun W. 3rd. Laboratory guide for identification of plant pathogenic bacteria. St Paul, Minnesota USA: APS Press; 2001.

13. Florencio C, Couri S, and Farina CS. Correlation between agar plate screening and solid-state fermentation for the prediction of cellulase production by *Trichoderma Strains*. Enzyme Research. 2012; Article ID 793708. 7 pages. doi: http://dx.doi.org/10.1155/2012/793708

14. Dellaporta SL, Wood J, and Hicks JB. A plant minipreparation: Version II. Plant molecular Biology Report.1983;1:19-20. doi: https://doi.org/10.1007/BF02712670

15. Weisburg WG, Barns SM, Pelletier DA, & Lane DJ. 16S ribosomal DNA amplification for phylogenetic study. Journal of Bacteriology. 1991; 173(2): 697–703. doi: https://www.ncbi.nlm.nih.gov/pmc/articles/PMC207061/

16. Barghouthi SA. A Universal Method for the Identification of Bacteria Based on General PCR Primers. Indian Journal of Microbiology. 2011; 51(4): 430–444. doi: http://doi.org/10.1007/s12088-011-0122-5

17. Altschul SF, Gish W, Miller W, Myers EW. & Lipman DJ. Basic local alignment search tool. J Mol Biol, 1990; 215:403–410. doi: https://doi.org/10.1016/S0022-2836(05)80360-2

18. Zerbino DR, y Birney E. Velvet: algorithms for de novo short read assembly using de Bruijn graphs. Genome research. 2008; 18(5): 821-9. doi: 10.1101/gr.074492.107

19. Gurevich A, Saveliev V, Vyahhi N, Tesler G. QUAST: quality assessment tool for genome assemblies. Bioinformatics. 2013; 29 (8): 1072-1075. doi: https://doi.org/10.1093/bioinformatics/btt086

bioRxiv preprint doi: https://doi.org/10.1101/2021.02.01.429127; this version posted February 1, 2021. The copyright holder for this preprint (which was not certified by peer review) is the author/funder, who has granted bioRxiv a license to display the preprint in perpetuity. It is made available under a CC-BY 4.0 International license.

20. Seemann T. Prokka: rapid prokaryotic genome annotation. Bioinformatics. 2014; 30(14): 2068–2069. doi: https://doi.org/10.1093/bioinformatics/btu153

21. Fouts DE, Mongodin EF, Mandrell RE, et al. Major structural differences and novel potential virulence mechanisms from the genomes of multiple campylobacter species. PLoS Biol. 2005;3(1):e15. doi:10.1371/journal.pbio.0030015

22. Lechner M, Findeiß S, Steiner L, Marz M, Stadler PF, Prohaska SJ. Proteinortho: Detection of (Co)orthologs in large-scale analysis. BMC Bioinformatics. 2011;12: 124. doi: https://doi.org/10.1186/1471-2105-12-124.

23. Wattam AR, Davis JJ, Assaf R, et al. Improvements to PATRIC, the all-bacterial Bioinformatics Database and Analysis Resource Center. *Nucleic Acids Res*. 2017;45(D1):D535-D542. doi:10.1093/nar/gkw1017

24. Pritchard L, Glover R, Humphris S, Elphinstone J, & Toth I. Genomics and Taxonomy in Diagnostics for Food Security: soft-rotting enterobacterial plant pathogens. Anal. Methods. 2015;8. doi: https://doi.org/10.1039/C5AY02550H

25. Moreno-Hagelsieb G, Latimer K. Choosing BLAST options for better detection of orthologs as reciprocal best hits. Bioinformatics. 2008;24(3):319-324. doi:10.1093/bioinformatics/btm585

26. Barajas HR, Romero MF, Martínez-Sánchez S, & Alcaraz LD. Global genomic similarity and core genome sequence diversity of the *Streptococcus* genus as a toolkit to identify closely related bacterial species in complex environments. PeerJ. 2019; *6*, e6233. doi: 10.7717/peerj.6233

27. Andrews S. FastQC: a quality control tool for high throughput sequence data. Available. 2010. online at: http://www.bioinformatics.babraham.ac.uk/projects/fastqc/

28. Kwon S, Lee B, Yoon S. CASPER: context-aware scheme for paired-end reads from high-throughput amplicon sequencing. BMC Bioinformatics. 2014; 15(Suppl 9):S10. doi: https://doi.org/10.1186/1471-2105-15-S9-S10

29. Li W, & Godzik A. Cd-hit: a fast program for clustering and comparing large sets of protein or nucleotide sequences. Bioinformatics. 2006; 22(13), 1658–1659. doi: https://doi.org/10.1093/bioinformatics/btl158

bioRxiv preprint doi: https://doi.org/10.1101/2021.02.01.429127; this version posted February 1, 2021. The copyright holder for this preprint (which was not certified by peer review) is the author/funder, who has granted bioRxiv a license to display the preprint in perpetuity. It is made available under a CC-BY 4.0 International license.

449 30. Caporaso JG, Kuczynski J, Stombaugh J, Bittinger K, Bushman FD, Costello EK, et al. QIIME allows
450 analysis of high-throughput community sequencing data. Nature methods. 2010;*7*(5):335–336. doi:
451 10.1038/nmeth.f.303
452 31. Alcaraz LD, Peimbert M, Barajas HR, Dorantes-Acosta AE, BowmanJL, & Arteaga-Vázquez MA.
453 Marchantia liverworts as a proxy to plants' basal microbiomes. Scientific reports. 2018;8(1): 12712. doi:
454 10.1038/s41598-018-31168-0
455 32. Haas BJ, Gevers D, Earl AM, et al. Chimeric 16S rRNA sequence formation and detection in Sanger and
456 454-pyrosequenced PCR amplicons. Genome Res. 2011; 21(3): 494–504. doi: 10.1101/gr.112730.110
457 33. McMurdie PJ, Holmes S. phyloseq: An R Package for Reproducible Interactive Analysis and Graphics of
458 Microbiome Census Data. PLoS ONE. 2013; 8(4): e61217. doi:
459 https://doi.org/10.1371/journal.pone.0061217
460 34. Narváez-Barragán DA, Tovar-Herrera OE, Torres M, Rodríguez M, Humphris S, Toth IK, Segovia L,
461 Serrano M, & Martínez-Anaya C. Expansin-like Exl1 from Pectobacterium is a virulence factor required
462 for host infection, and induces a defence plant response involving ROS, and jasmonate, ethylene and
463 salicylic acid signalling pathways in *Arabidopsis thaliana*. Scientific Reports. 2020. 10(1), 7747.
464 https://doi.org/10.1038/s41598-020-64529-9
465 35. Dees MW, Lysøe E, Rossmann S, Perminow J, Brurberg MB. *Pectobacterium Polaris* sp. nov., isolated
466 from potato (*Solanum tuberosum*). Int J Syst Evol Microbiol. 2017b; 67: 5222–5229. doi:
467 https://doi.org/10.1099/ijsem.0.002448
468 36. Portier P, Pédron J, Taghouti G, Fischer-Le Saux M, Caullireau E, Bertrand C. et al., Elevation of
469 *Pectobacterium carotovorum* subsp. *Odoriferum* to species level as *Pectobacterium odoriferum* sp. nov.,
470 proposal of *Pectobacterium brasiliense* sp. nov. and *Pectobacterium actinidiae* sp. nov., emended
471 description of *Pectobacterium carotovorum* and description of *Pectobacterium versatile* sp. nov., isolated
472 from streams and symptoms on diverse plants. Int J Syst Evol Microbiol. 2019; *6*9(10): 3207–3216. doi:
473 https://doi.org/10.1099/ijsem.0.003611
474 37. Rost B. Twilight zone of protein sequence alignments. Protein Eng Des Sel. 1999;12: 85–94.
475 doi:10.1093/protein/12.2.85

bioRxiv preprint doi: https://doi.org/10.1101/2021.02.01.429127; this version posted February 1, 2021. The copyright holder for this preprint (which was not certified by peer review) is the author/funder, who has granted bioRxiv a license to display the preprint in perpetuity. It is made available under a CC-BY 4.0 International license.

476 38. Torres-Bojórquez, Ariana Isabel, Cervantes-Díaz, Lourdes, Núñez-Ramírez, Fidel, Morales-Maza,
477 Antonio, & Samaniego-Gámez, Blancka Yesenia. Primer reporte de *Pectobacterium* spp. asociada a
478 *Opuntia ficus* en Baja California, México. Idesia (Arica). 2016. *34*(4), 69-71.
479 https://dx.doi.org/10.4067/S0718-34292016005000015
480 39. Corrales García J, Valdez C. Nopalitos y tunas, producción, comercialización, poscosecha e
481 industrialización. 2003.
482 40. Yahia E, Saenz C. Cactus pera (especie Opuntia). 2011. págs. 290–329. doi: 10.1533 /
483 9780857092762.290
484 41. Alcorn SM, Orum TV, Steigerwalt AG, Foster JL, Fogleman JC, Brenner DJ. Taxonomy and
485 pathogenicity of *Erwinia cacticida* sp. nov. *Int J Syst Bacteriol*. 1991;41(2):197-212.
486 doi:10.1099/00207713-41-2-197
487 42. Kõiv V, Roosaare M, Vedler E, Kivistik PA, Toppi K, Schryer DW., et al. Microbial population dynamics
488 in response to *Pectobacterium atrosepticum* infection in potato tubers. Sci. Rep. 2015;5:11606. doi:
489 https://doi.org/10.1038/srep11606
490 43. Fonseca-García C, Coleman-Derr D, Garrido E, Visel A, Tringe SG, & Partida-Martínez LP. The Cacti
491 Microbiome: Interplay between Habitat-Filtering and Host-Specificity. Frontiers in microbiology. 2016;
492 *7*: 150. doi: https://doi.org/10.3389/fmicb.2016.00150
493 44. Voronina OL, Kunda MS, Ryzhova NN, Aksenova EI, Semenov AN, Lasareva A V, et al. The Variability
494 of the Order Burkholderiales Representatives in the Healthcare Units. Lyubetsky V, editor. Biomed Res
495 Int.2015; 680210. doi:10.1155/2015/680210
496 45. Abraham W-R, Rohde M, Bennasar A. The Family Caulobacteraceae BT - The Prokaryotes:
497 Alphaproteobacteria and Betaproteobacteria. In: Rosenberg E, DeLong EF, Lory S, Stackebrandt E,
498 Thompson F, editors. Berlin, Heidelberg: Springer Berlin Heidelberg; 2014. pp. 179–205. doi:
499 https://doi.org/10.1007/978-3-642-30197-1_259
500 46. Schweitzer B, Huber I, Amann R, Ludwig W, & Simon M. Alpha- and beta-Proteobacteria control the
501 consumption and release of amino acids on lake snow aggregates. Appl. Environ. Microbiol. 2001;
502 *67*(2):632–645. doi: 10.1128/AEM.67.2.632-645.2001

bioRxiv preprint doi: https://doi.org/10.1101/2021.02.01.429127; this version posted February 1, 2021. The copyright holder for this preprint (which was not certified by peer review) is the author/funder, who has granted bioRxiv a license to display the preprint in perpetuity. It is made available under a CC-BY 4.0 International license.

Supporting information

S1 Figure. Circular representation of the genomes of Pectobacterium strain A1 and A3. Concentric circles represent genomic data, from the outermost circle to the innermost: size in Mbp, Contigs, forward strand predicted Coding sequences (CDS), reverse strand CDS, predicted antibiotic resistance genes, virulence genes, transporter genes, G-C content, G-C skew, and unmerged gene clusters identified by PATRIC suite. Contigs were aligned and reordered using the complete genome of type strain *P. carotovorum subsp. brasiliensis* BC1 as a reference for strain A1 and the strain *P. polaris* NIBIO1392 as a reference for strain A3. Those contigs unable to align were placed at the end (red bar).

(TIF)

S1 Table. Sequences used in this study

(XLSX)

S2 Table. ANI identity values. The green rows indicate *Pectobacterium brasiliense*, the purple rows indicate *Pectobacterium polaris*, the yellow ones indicate *Pectobacterium carotovorum*, the blue column indicates isolate A3_Tetetzo and the red one indicates isolate A1_Tetetzo.

(XLSX)

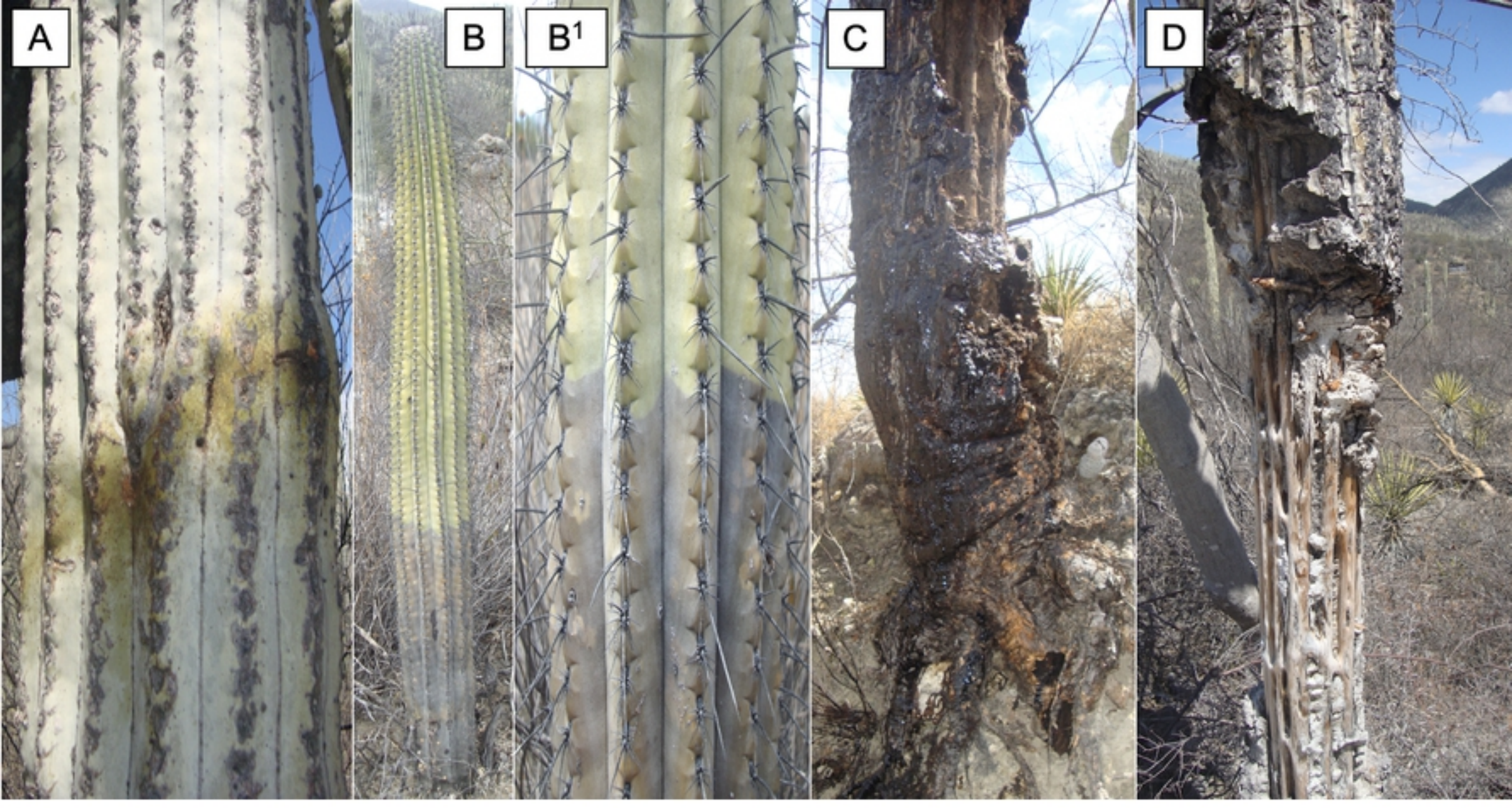


Figure 1

bioRxiv preprint doi: https://doi.org/10.1101/2021.02.01.429127; this version posted February 1, 2021. The copyright holder for this preprint (which was not certified by peer review) is the author/funder, who has granted bioRxiv a license to display the preprint in perpetuity. It is made available under a CC-BY 4.0 International license.

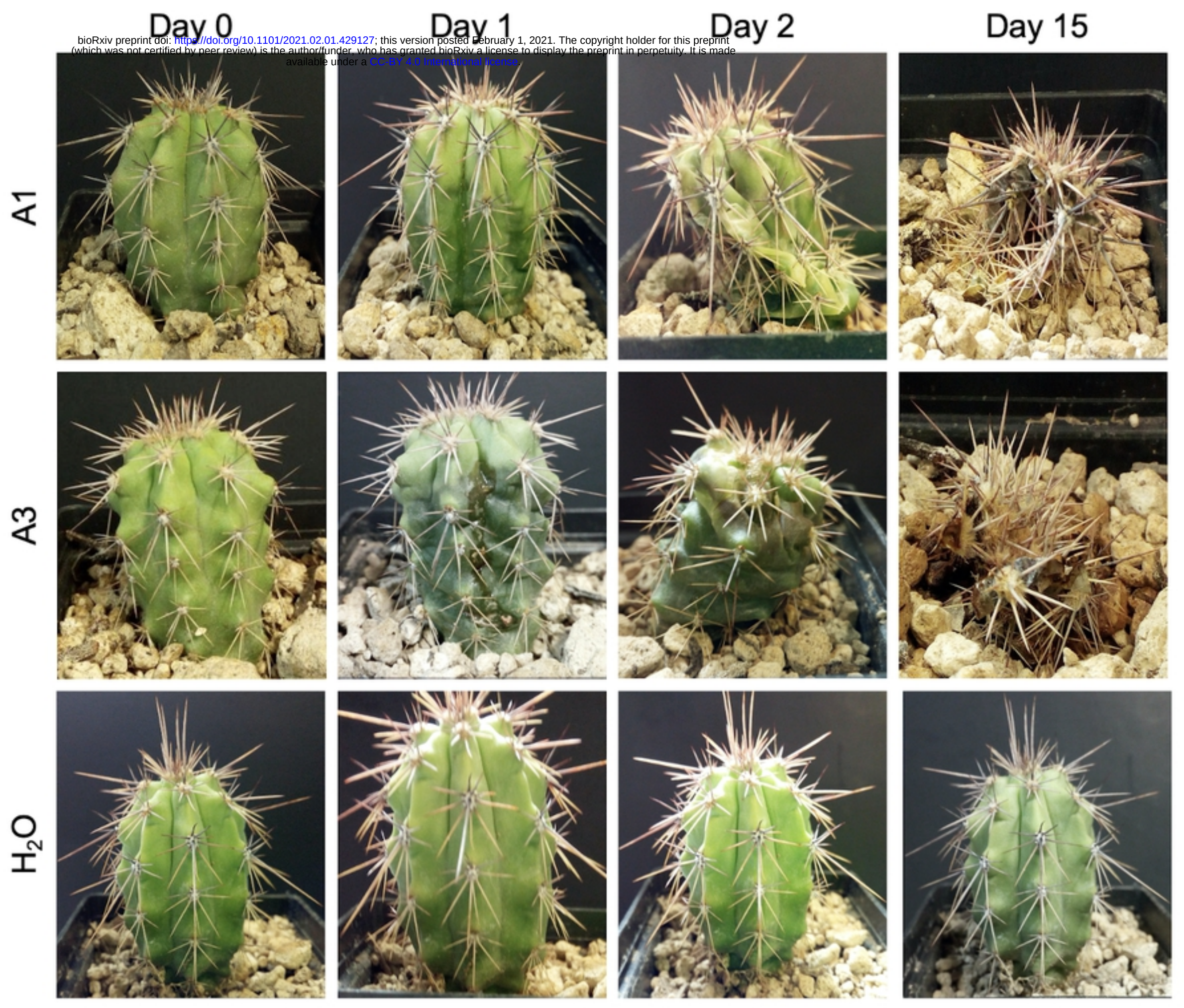


Figure 2

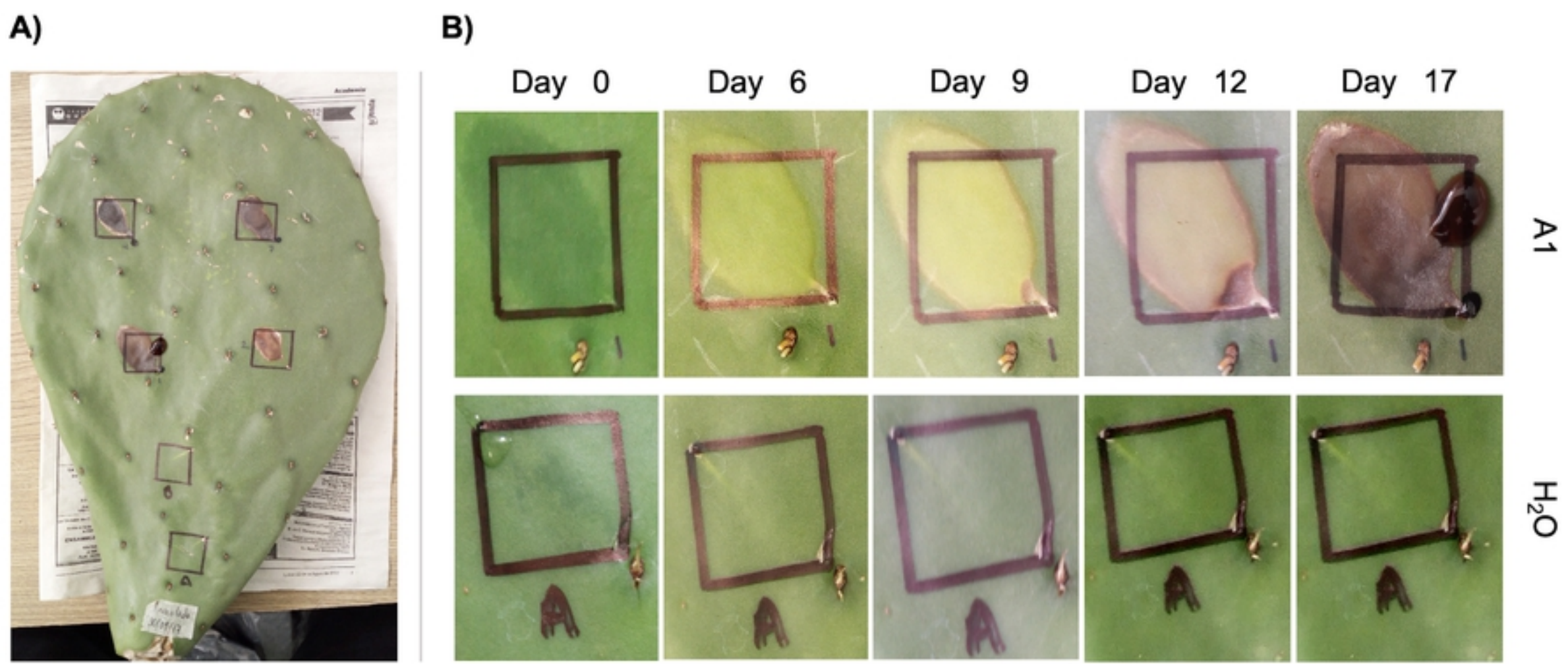


Figure 3

bioRxiv preprint doi: https://doi.org/10.1101/2021.02.01.429127; this version posted February 1, 2021. The copyright holder for this preprint (which was not certified by peer review) is the author/funder, who has granted bioRxiv a license to display the preprint in perpetuity. It is made available under a CC-BY 4.0 International license.

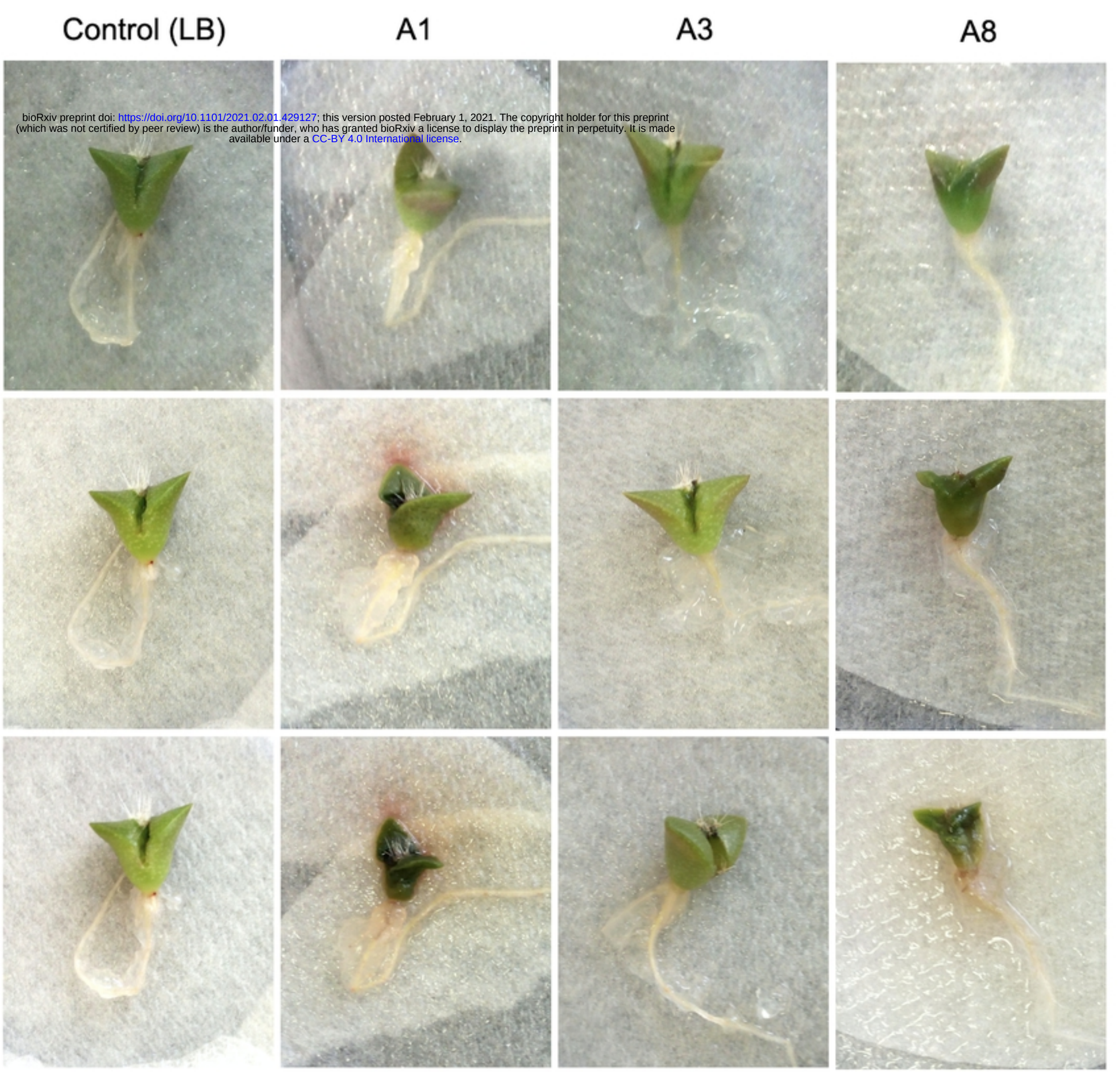


Figure 4

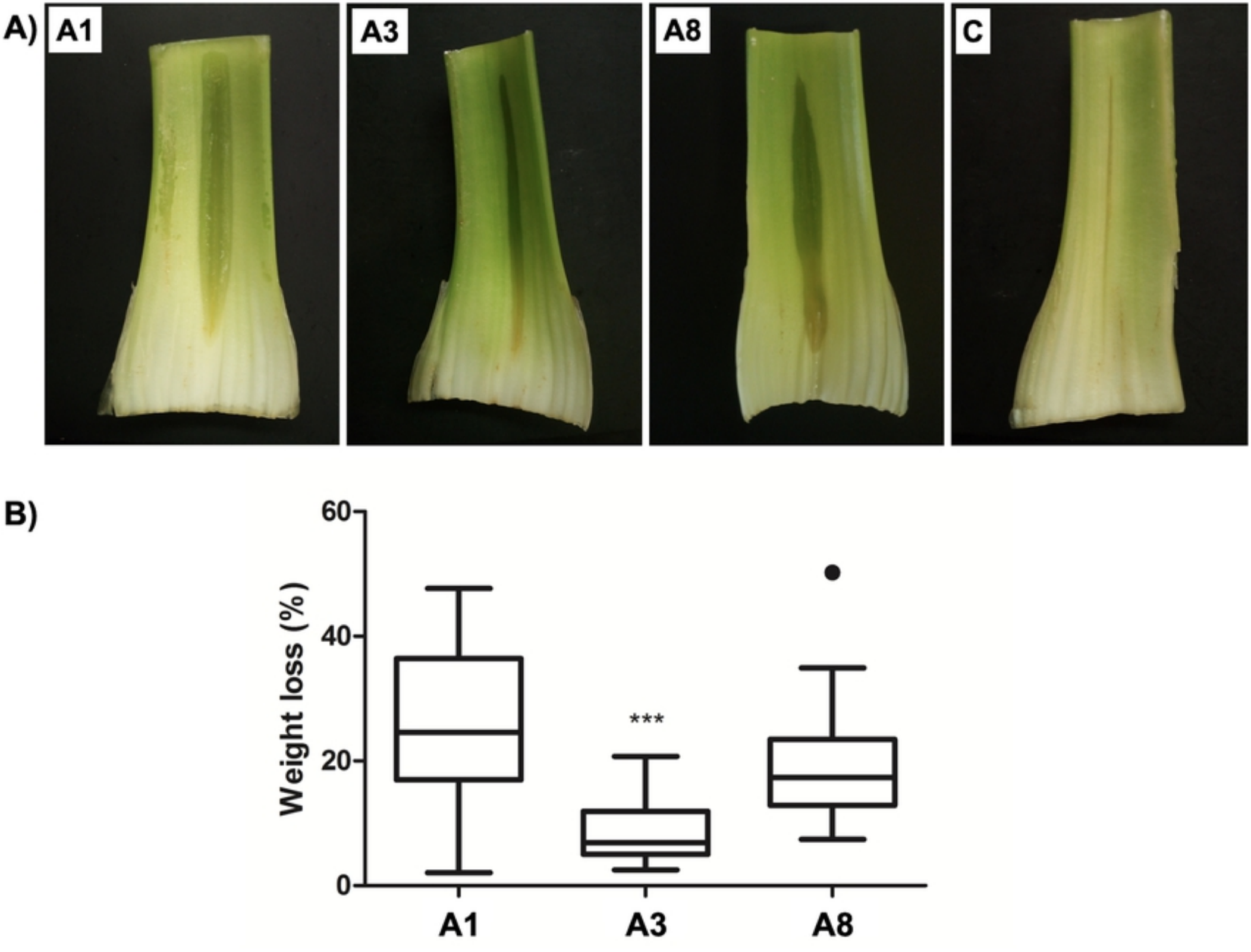


Figure 5

bioRxiv preprint doi: https://doi.org/10.1101/2021.02.01.429127; this version posted February 1, 2021. The copyright holder for this preprint (which was not certified by peer review) is the author/funder, who has granted bioRxiv a license to display the preprint in perpetuity. It is made available under a CC-BY 4.0 International license.

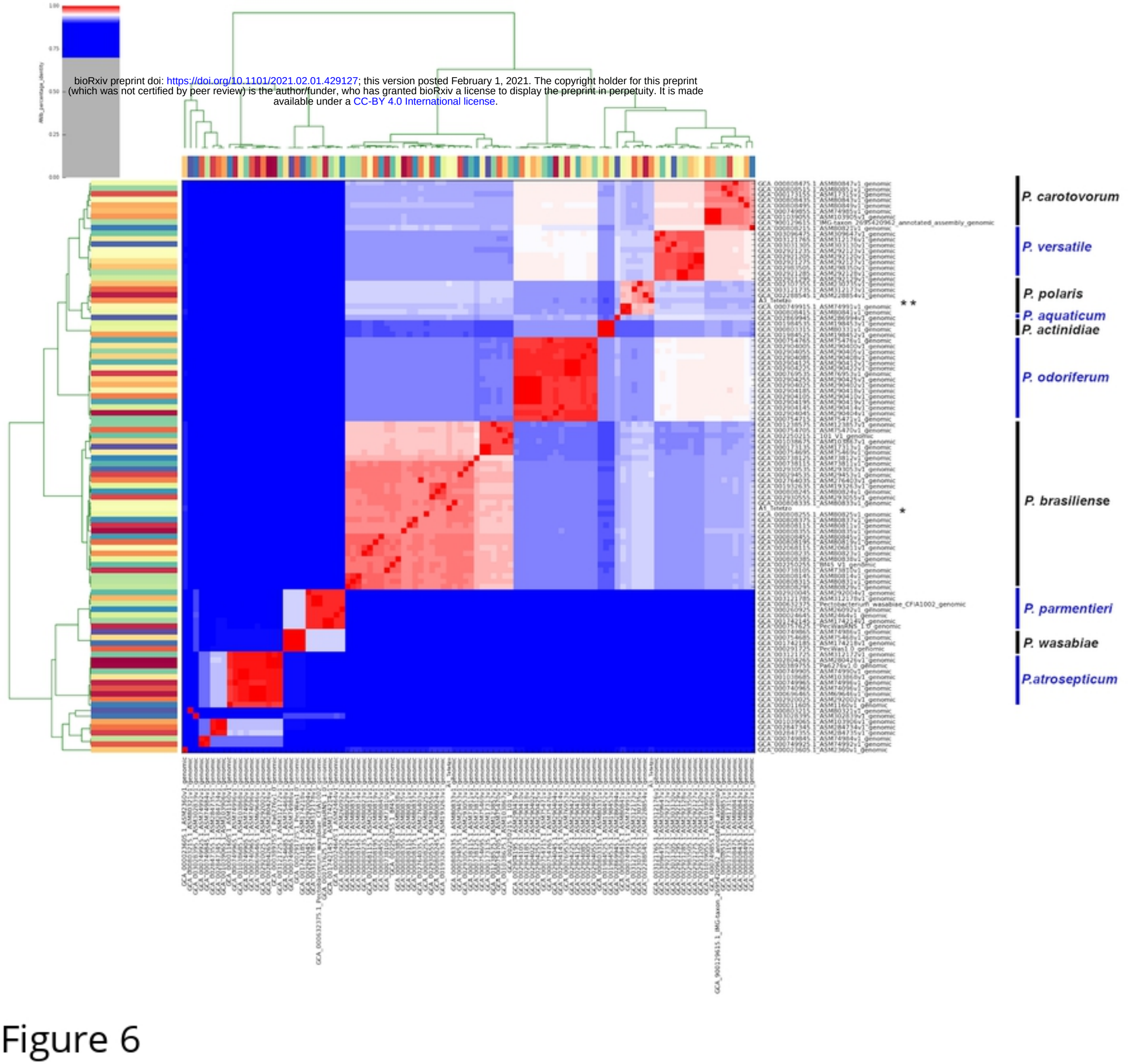
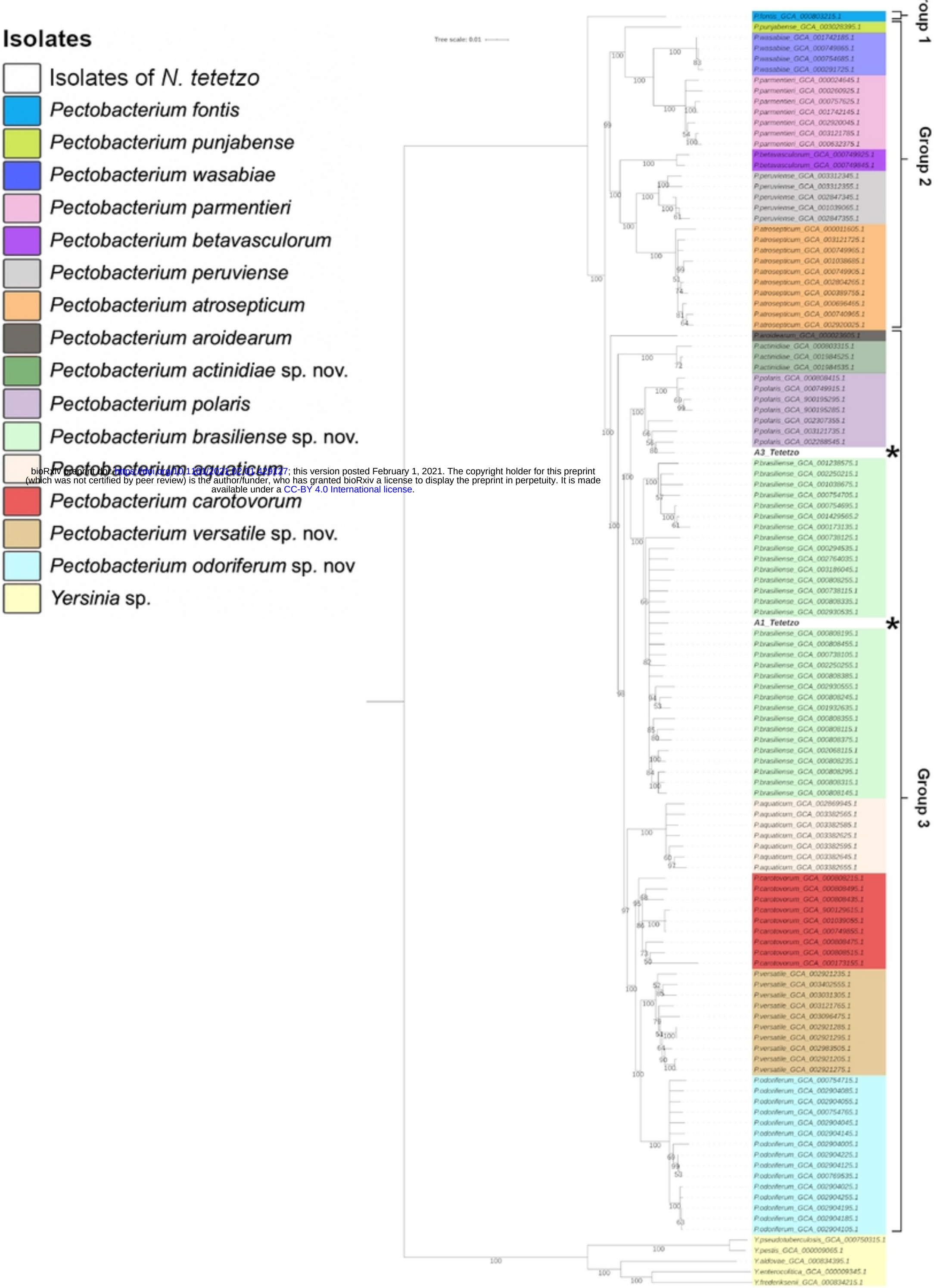


Figure 6

GGS Dendogram



bioRxiv preprint doi: https://doi.org/10.1101/2021.02.01.429127; this version posted February 1, 2021. The copyright holder for this preprint (which was not certified by peer review) is the author/funder, who has granted bioRxiv a license to display the preprint in perpetuity. It is made available under a CC-BY 4.0 International license.

Figure 7

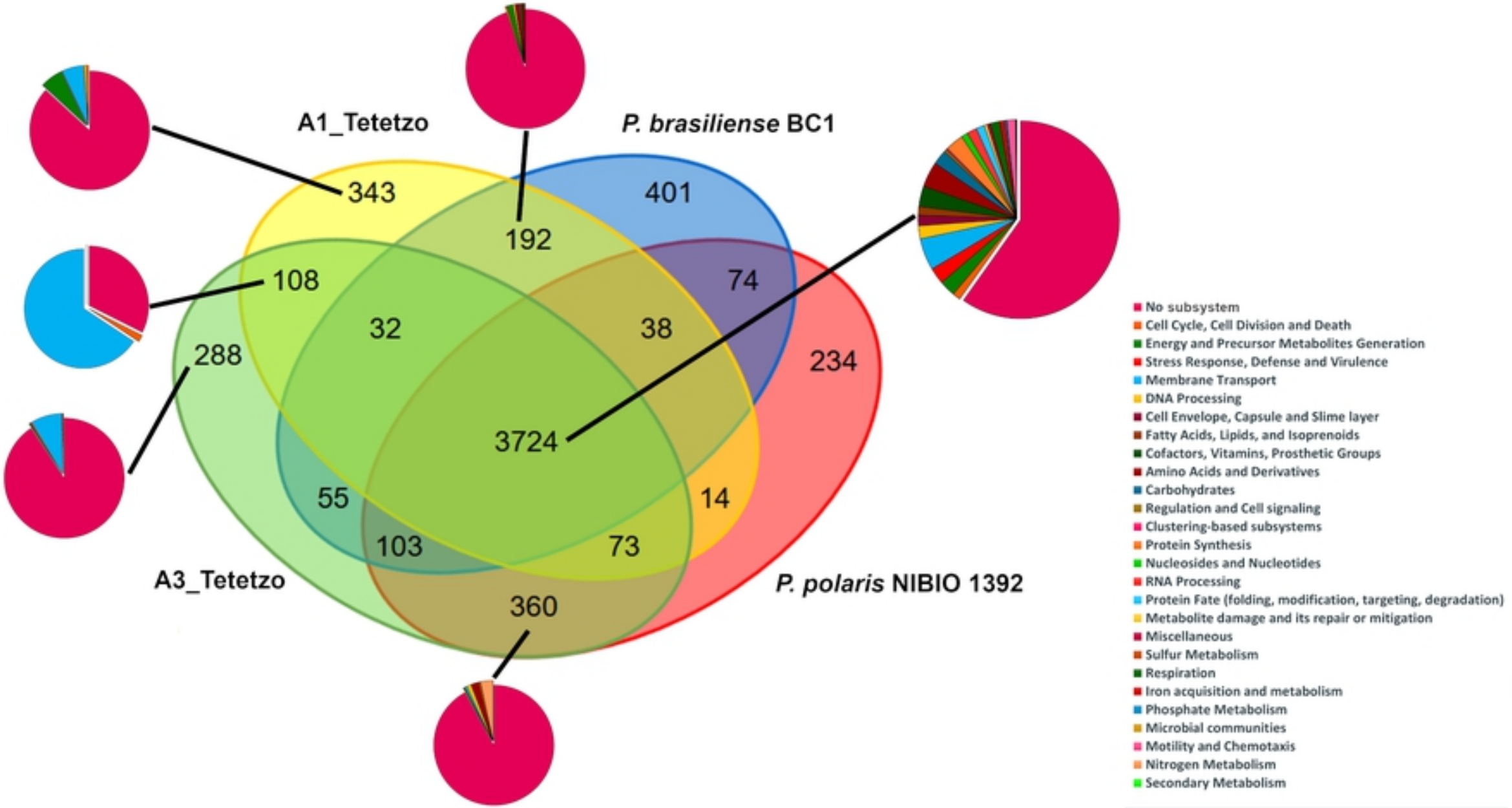

A1_Tetetzo
P. brasiliense BC1
A3_Tetetzo
P. polaris NIBIO 1392
343
401
192
108
74
32
38
288
234
3724
55
14
103
73
360
No subsystem
Cell Cycle, Cell Division and Death
Energy and Precursor Metabolites Generation
Stress Response, Defense and Virulence
Membrane Transport
DNA Processing
Cell Envelope, Capsule and Slime layer
Fatty Acids, Lipids, and Isoprenoids
Cofactors, Vitamins, Prosthetic Groups
Amino Acids and Derivatives
Carbohydrates
Regulation and Cell signaling
Clustering-based subsystems
Protein Synthesis
Nucleosides and Nucleotides
RNA Processing
Protein Fate (folding, modification, targeting, degradation)
Metabolite damage and its repair or mitigation
Miscellaneous
Sulfur Metabolism
Respiration
Iron acquisition and metabolism
Phosphate Metabolism
Microbial communities
Motility and Chemotaxis
Nitrogen Metabolism
Secondary Metabolism

Figure 8

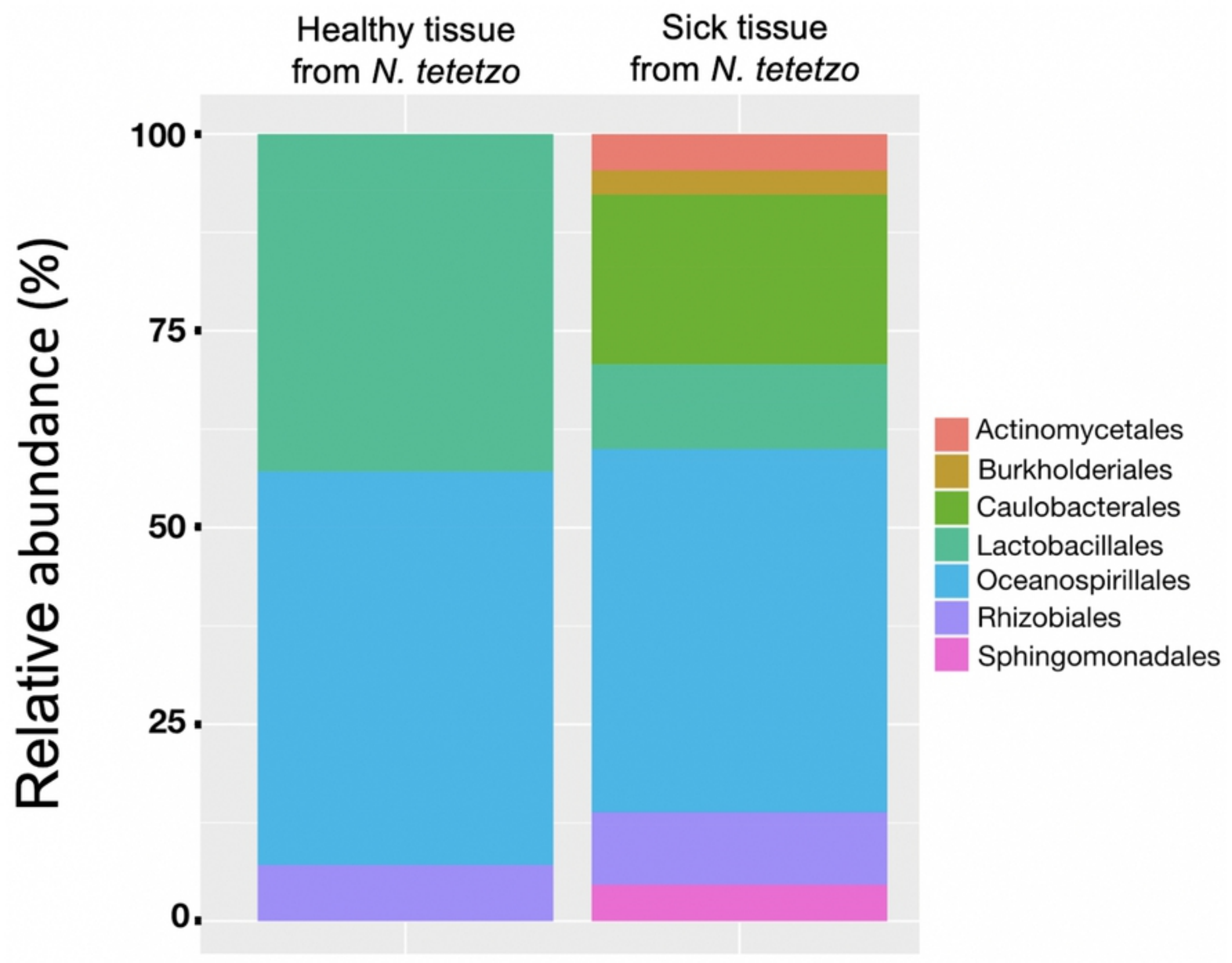

Healthy tissue
from N. tetetzo
Sick tissue
from N. tetetzo
Relative abundance (%)
100
75
50
25
0
Actinomycetales
Burkholderiales
Caulobacterales
Lactobacillales
Oceanospirillales
Rhizobiales
Sphingomonadales

Figure 9